

Buckling disappearance via merging/divergence in a nonlinear three-d.o.f. system with linear constitutive law

Angelo Luongo*, Manuel Ferretti

Department of Civil, Construction-Architectural and Environmental Engineering, University of L'Aquila, 67100 L'Aquila, Italy

ARTICLE INFO

Keywords:

Spherical pendulum
Bifurcation from a non-trivial path
Buckling disappearance
Merging of the eigenvalues
Divergence of the critical load

ABSTRACT

The phenomenon of buckling disappearance, occurring in a parameter-dependent family of systems admitting a nontrivial fundamental path, is studied. Two different forms of disappearance are detected, namely: (i) the *divergence*, in which the critical load continuously tends to infinity, and (ii) the *merging*, in which two critical loads approach each other, coalesce, and then disappear at a finite value of the critical load. It is shown that the two phenomena can be exhibited by the same mechanical system, when a suitable elasto-geometric parameter is varied. More importantly, it is proved that merging continuously changes into divergence when a second parameter is changed. A paradigmatic system is chosen to illustrate the two forms of buckling, *i.e.*, a three degree-of-freedom spherical pendulum, elastically constrained at the ground, loaded by a transverse force and/or a conservative couple, made of two longitudinal potential forces. The springs are taken elastically linear, to stress the fact that divergence not necessarily calls for introducing a nonlinear constitutive law, as also mentioned in literature. Only a linear bifurcation analysis is carried out here, aimed to find the bifurcation points along the nonlinear fundamental path. However, due to the presence of non-negligible prestrains, such a bifurcation problem is governed by nonlinear algebraic equations, whose number of roots cannot be predicted in advance.

1. Introduction

Several papers have recently appeared in literature concerning the effects of precritical nonlinearities on buckling of elastic structures [1–4]. This aspect assumes particular importance in the field of biomechanics, where buckling of very soft biological tissues is strongly affected by prestrains [5,6]. Some of these papers were inspired by the paradigmatic two degree-of-freedom Feodosyev model [7] (or its variants), constituted by a reverse pendulum, axially deformable and elastically constrained at the ground, compressed by a gravitational force. It is easily proved for this model that, when the axial-to-flexural stiffness ratio is progressively reduced, buckling disappears at a critical value of the ratio. Such a phenomenon was detailed commented in [8], where the notion of *merging* of the eigenvalues (each of which representing a buckling load), as opposite to *crossing* of eigenvalues, was given. Namely, merging means that when a physical parameter is varied (the stiffness ratio, in this case), two distinct buckling loads approach each other, coalesce and then disappear in the real field. The mechanism, noticeably, is the same occurring in the analysis of dynamic (or flutter) bifurcation of nonconservative systems, in which two real frequencies coalesce and then become complex conjugate [9]. It was, moreover, stressed in [8], that merging is strictly related to the

existence of precritical strains, which make the elastic and geometric stiffness matrices load-dependent. This entails that the *linear bifurcation* (*i.e.*, the analysis of the branch points, and not the construction of the bifurcated paths) is, indeed, governed by a *nonlinear* eigenvalue problem. In contrast, when precritical strains are neglected, only crossing can manifest itself, according to which two eigenvalues coalesce and then survive, with exchanged order, when the physical parameter is varied through a threshold value. In this context, interesting systems exhibiting the disappearance of buckling loads and restabilization can be found in [10,11] for variable-length one-dimensional structures, and in [12–14] for membrane wrinkling.

In a successive paper [15], the (beneficial) effects of precritical nonlinearities on a continuous model of fixed-free beam were investigated. There, the beam suffers of lateral instability induced by transverse forces and a conservative couple. It was proved that, by keeping fixed the out-of-plane flexural and torsional stiffnesses, while reducing the in-plane flexural stiffness, the buckling values of the load/couple increase, tending to infinity at a value of the in-plane stiffness. Such a phenomenon is often referred in literature as a *divergence* (of the critical load) [15]. Of course, merging and divergence have the same practical consequences, *i.e.*, buckling disappears at a threshold value

* Corresponding author.

E-mail addresses: angelo.luongo@univaq.it (A. Luongo), manuel.ferretti@univaq.it (M. Ferretti).

of a physical parameter, but they are intrinsically different, since the former entails a sudden disappearance at a finite load, while the latter entails a fading at infinitely large loads. The reasons for the occurrence of a different mechanism of disappearance were not explained in [15], but left for future work.

On the other hand, there exist in literature a few papers discussing the role of the elastic law on these phenomena. In [16], by dealing with the Euler beam, it was observed that, by introducing a softening effect in the elastic material behavior, the reduced pre-buckling length is more than compensated by a softening of the elastic response, so that a reduction (instead of a magnification) of the Euler critical load is found. A similar approach has been more extensively developed in [6], where it has been proved and corroborated by experimental tests, that, by using the Ogden-Hill law, the Feodosyev ‘paradox’ (in their nomenclature) is removed, in the sense that two degree-of-freedom system buckles at any small value of the axial stiffness, but at increasingly large values of the compressive load. In the nomenclature proposed here, it could be said that the merging phenomenon, occurring for a linear constitutive law, is modified into a divergence phenomenon when the constitutive law is made nonlinear. Additional interesting results are discussed in [6], relevant to *tensile buckling* of simple structures, obtained by introducing prestrains in a rod with an internal slider, firstly introduced in [17], also showing divergence. A more extensive analysis has been carried out in [5], where results relevant to chains of internally sliding rods are studied, again manifesting divergence.

To the state-of-art, therefore, it is not clear: (i) if merging and divergence manifest themselves in different systems, or, in contrast, they can coexist in a given family of systems when one or more auxiliary parameter are varied; (ii) if it is really mandatory to introduce a (although more realistic) nonlinear constitutive law, or, instead, the same phenomena can be observed in structures with linear constitutive law. This paper aims to address both questions. To this end, a paradigmatic three degrees-of-freedom system, made of a spherical pendulum elastically grounded by *linear springs*, loaded by transverse forces and a couple, is considered, reproducing, at the better extent, the behavior of the fixed-free beam studied in [15]. The pendulum experiences an in-plane large deflection described by the load-rotation fundamental path, from which the structure bifurcates in a flexural–torsional-like pattern. Goal of the paper is to show that, in spite of the linearity of the elastic law, the system exhibit *divergence as well as merging*, when some parameters and/or the type of load is changed. More remarkably, it will be shown that, by browsing a two-parameter family of systems, one passes continuously from a form of disappearance to another.

The paper is organized as follows. In Section 2 the nonlinear model is derived. In Section 3 the nonlinear fundamental path is studied, in asymptotic approximate form and in a numeric exact form. In Section 4 a linear bifurcation analysis along the nonlinear fundamental path is carried out, calling for solving a nonlinear eigenvalue problem. Here, a parametric analysis is performed. Finally, in Section 5, some conclusions are drawn and new research perspectives outlined.

2. Model

A three-d.o.f. system is considered, made of a spherical rigid pendulum of length ℓ , initially oriented in the $\bar{\mathbf{a}}_x$ direction of a 3D space spanned by the triad $(\bar{\mathbf{a}}_x, \bar{\mathbf{a}}_y, \bar{\mathbf{a}}_z)$ (Fig. 1a).

The pendulum, at its left end A , is hinged at the ground by a Cardanic joint (namely, an in-series assembly of three mutually orthogonal cylindrical hinges, Fig. 1a), equipped with torsional elastic springs k_x, k_y, k_z reacting to rotations around the *current* axes of the joint. The system is loaded at the right end B by a transverse force $P\bar{\mathbf{a}}_y$ and two equal and opposite longitudinal forces $\pm F\bar{\mathbf{a}}_x$, constituting a *configuration-dependent* conservative couple C (see, e.g., [18]). All the forces are applied at points rigidly connected at the point B , namely: (i) P is applied at $B_0 := \ell\bar{\mathbf{a}}_x + e\bar{\mathbf{a}}_y$, with $e \geq 0$ the eccentricity, and (ii) the forces $\pm F$ are applied at points $B_{1,2} = \ell\bar{\mathbf{a}}_x \mp \frac{d}{2}\bar{\mathbf{a}}_y$ with $d > 0$ the initial arm of the couple.

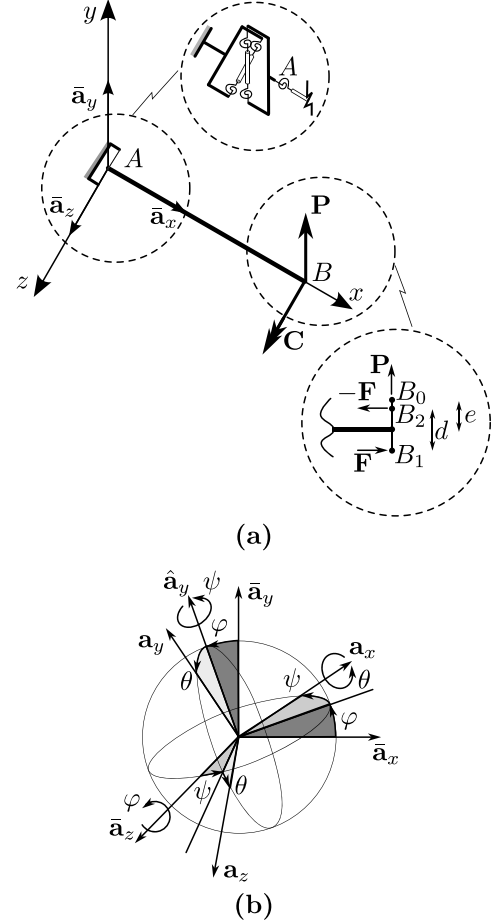


Fig. 1. Model: rigid pendulum hinged by a Cardanic joint: (a) system and forces, (b) Cardan angles.

Kinematics. The current position of the pendulum is defined by the three Cardan angles (φ, ψ, θ) (Fig. 1b), which are the amplitudes of rotations successively impressed around: (i) the $\bar{\mathbf{a}}_z$ axis, (ii) the transformed direction $\hat{\mathbf{a}}_y$ of the $\bar{\mathbf{a}}_y$ axis, and (iii) the final position \mathbf{a}_x of the $\bar{\mathbf{a}}_x$ axis. The rotation is described by the tensor [19]:

$$\mathbf{R} = \begin{bmatrix} \cos \psi \cos \varphi & \sin \theta \sin \psi \cos \varphi & \cos \theta \sin \psi \cos \varphi \\ \cos \psi \sin \varphi & -\cos \theta \sin \varphi & +\sin \theta \sin \varphi \\ \sin \psi & \sin \theta \cos \psi & \cos \theta \cos \psi \end{bmatrix} \quad (1)$$

which leads the reference triad $(\bar{\mathbf{a}}_x, \bar{\mathbf{a}}_y, \bar{\mathbf{a}}_z)$ to match the current triad $(\mathbf{a}_x, \mathbf{a}_y, \mathbf{a}_z)$; hence, $\mathbf{a}_\alpha = \mathbf{R}\bar{\mathbf{a}}_\alpha$ with $\alpha = x, y, z$.

The displacement of points B_0, B_1, B_2 , are:

$$\mathbf{u}_{B_0} = (\mathbf{R} - \mathbf{I})(\ell\bar{\mathbf{a}}_x + e\bar{\mathbf{a}}_y) \quad (2a)$$

$$\mathbf{u}_{B_{1,2}} = (\mathbf{R} - \mathbf{I})\left(\ell\bar{\mathbf{a}}_x \mp \frac{d}{2}\bar{\mathbf{a}}_y\right) \quad (2b)$$

Equilibrium equations. The elastic potential energy is:

$$U := \frac{1}{2}(k_z\varphi^2 + k_y\psi^2 + k_x\theta^2) \quad (3)$$

The potential energy of the forces, by making use of Eqs. (1) and (2), and to within an inessential constant, is:

$$V := -P \bar{\mathbf{a}}_y \cdot \mathbf{u}_{B_0} - F \bar{\mathbf{a}}_x \cdot (\mathbf{u}_{B_1} - \mathbf{u}_{B_2})$$

$$= -P [\ell \cos \psi \sin \varphi + e (\sin \theta \sin \psi \sin \varphi + \cos \theta \cos \varphi)]$$

$$+ C (\sin \theta \sin \psi \cos \varphi - \cos \theta \sin \varphi) \quad (4)$$

where $C := Fd$ is the value of the couple in the reference configuration. By introducing the nondimensional quantities:

$$\alpha := \frac{k_x}{k_z}, \quad \beta := \frac{k_y}{k_z}, \quad \eta := \frac{e}{\ell}, \quad \mu := \frac{P\ell}{k_z}, \quad \nu := \frac{C}{k_z} \quad (5)$$

the Total Potential Energy (TPE) of the system, $\Pi := U + V$, reads:

$$\Pi = k_z \left\{ \frac{1}{2} (\varphi^2 + \beta \psi^2 + \alpha \theta^2) - \mu [\cos \psi \sin \varphi + \eta (\sin \theta \sin \psi \sin \varphi + \cos \theta \cos \varphi)] + \nu (\sin \theta \sin \psi \cos \varphi - \cos \theta \sin \varphi) \right\} \quad (6)$$

By making the TPE stationary with respect to the Lagrangian parameters (φ, ψ, θ) , the equilibrium equations follow:

$$\varphi - \mu [\cos \psi \cos \varphi + \eta (\sin \theta \sin \psi \cos \varphi - \cos \theta \sin \varphi)] - \nu (\sin \theta \sin \psi \sin \varphi + \cos \theta \cos \varphi) = 0 \quad (7a)$$

$$\beta \psi + \mu [\sin \psi \sin \varphi - \eta \sin \theta \cos \psi \sin \varphi] + \nu \sin \theta \cos \psi \cos \varphi = 0 \quad (7b)$$

$$\alpha \theta - \mu \eta (\cos \theta \sin \psi \sin \varphi - \sin \theta \cos \varphi) + \nu (\cos \theta \sin \psi \cos \varphi + \sin \theta \sin \varphi) = 0 \quad (7c)$$

The parameters α, β appearing in Eq. (5) will be referred to as the out-of-plane stiffnesses of the pendulum, namely the torsional and flexural stiffnesses, respectively. The parameters μ, ν as the load-parameters, namely the force and the couple, respectively. The nomenclature understood that, when considering a family of systems, the in-plane stiffness k_z is kept constant. Accordingly, α, β large denote (out-of-plane) stiff systems, while α, β small denote (out-of-plane) soft systems.

3. Fundamental path

The equilibrium Eq. (7) admit a *planar solution* $\varphi = \hat{\varphi}(\mu, \nu)$, $\psi = \hat{\theta} = 0$, in which the pendulum rotates in the vertical $(\bar{\mathbf{a}}_x, \bar{\mathbf{a}}_y)$ plane. Equilibrium is governed by:

$$\hat{\varphi} - (\mu + \nu) \cos \hat{\varphi} + \mu \eta \sin \hat{\varphi} = 0 \quad (8)$$

whose solutions describe the *fundamental path* of the system (i.e., a surface in the $(\hat{\varphi}, \mu, \nu)$ space, or a curve if just one load acts on the pendulum).

Eq. (8) differs from that of the linear theory (which does not account for displacements in the equilibrium condition), i.e., $\hat{\varphi}_L := \mu + \nu$. In fact, Eq. (8) accounts for the reduction with $\hat{\varphi}$ of the arm of the force with respect A as well as of the arm of the couple. Hence, the fundamental path is non-trivial and nonlinear. The graphic construction in Fig. 2 shows that, if the nondimensional loads μ and ν are small enough (curve 1), there exist a unique solution; in contrast, if μ, ν are large enough (curve 2), there exist more than one solution. However, here the interest is limited to positive angles of maximum amplitude close to $\frac{\pi}{2}$, as it will appear clear soon, where just one solution exists.

When $\mu = 0$, Eq. (8) admits the solution:

$$\nu = \frac{\hat{\varphi}}{\cos \hat{\varphi}} \quad (9)$$

and when $\nu = 0$:

$$\mu = \frac{\hat{\varphi}}{\cos \hat{\varphi} - \eta \sin \hat{\varphi}} \quad (10)$$

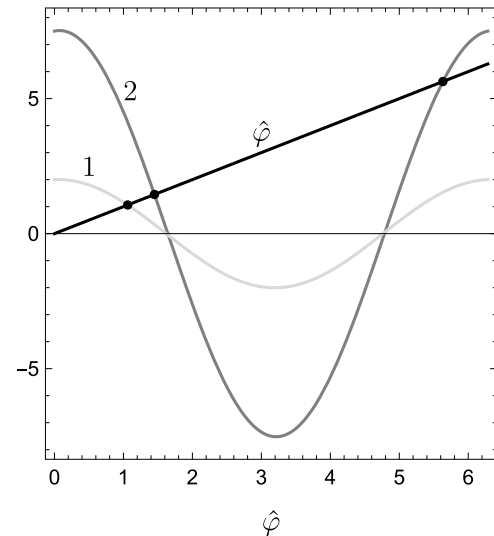


Fig. 2. Solutions to Eq. (8), rewritten as $\hat{\varphi} = f(\hat{\varphi}; \mu, \nu)$; curve 1: small loads $\mu = 1, \nu = 1$ and $\eta = -0.1$ (one solution), curve 2: large loads $\mu = 5.5, \nu = 2$ and $\eta = -0.1$ (more solutions).

both plotted in Figs. 3a,b.

It is seen (Fig. 3a) that when $\hat{\varphi} \rightarrow \frac{\pi}{2}$ then $\nu \rightarrow \infty$; at this angle, indeed, the arm of the couple is zero, so that, for equilibrium with the elastic reaction, the magnitude of the couple must be infinitely large. Similarly (Fig. 3b), if $\eta = 0$, when $\hat{\varphi} \rightarrow \frac{\pi}{2}$ then $\mu \rightarrow \infty$, since in this configuration the vertical force P has zero arm with respect to the grounded hinge. However, the asymptote moves to lower values when $\eta > 0$ (and to higher values when $\eta < 0$, not displayed) at which the previous alignment occurs, so that the interval of interest is $(0, \frac{\pi}{2} - \arctan(\eta))$.

Eq. (8) cannot be solved in closed form to give the rotation as function of the loads, i.e., $\hat{\varphi} = \hat{\varphi}(\mu, \nu)$, not even for just one load acting. However, by applying a perturbation method for $\hat{\varphi}, \mu, \nu$ small (details omitted), the following approximate solution is found:

$$\hat{\varphi} = (\mu + \nu)(1 - \eta \mu) + \frac{1}{2}(\mu + \nu) [2\eta^2 \mu^2 - (\mu + \nu)^2] + \dots \quad (11)$$

which, for the two loads acting separately, reduces to:

$$\hat{\varphi} = \begin{cases} \nu - \frac{1}{2}\nu^3 + \dots & \text{when } \mu = 0 \\ \mu - \eta\mu^2 + \left(\eta^2 - \frac{1}{2}\right)\mu^3 + \dots & \text{when } \nu = 0 \end{cases} \quad (12)$$

On the other hand, asymptotic expansions for large $\hat{\varphi}, \mu, \nu$ (with η still kept to be small in modulus), and therefore holding close to the asymptots, can also be obtained (details omitted). They are found to assume the following form:

$$\hat{\varphi} = \frac{\pi}{2} \left(1 - \frac{1}{\mu + \nu} \right) - \eta \frac{\mu}{\mu + \nu} + \dots \quad (13)$$

which, specialized to the case of loads acting separately, reads:

$$\hat{\varphi} = \begin{cases} \frac{\pi}{2} \left(1 - \frac{1}{\nu} \right) + \dots & \text{when } \mu = 0 \\ \frac{\pi}{2} \left(1 - \frac{1}{\mu} \right) - \eta + \dots & \text{when } \nu = 0 \end{cases} \quad (14)$$

The asymptotic solutions in Eqs. (12) and (14) are plotted in Figs. 3a,b and compared with the exact solutions. It is seen that the approximation is acceptable only for very small or large values of the load parameters.

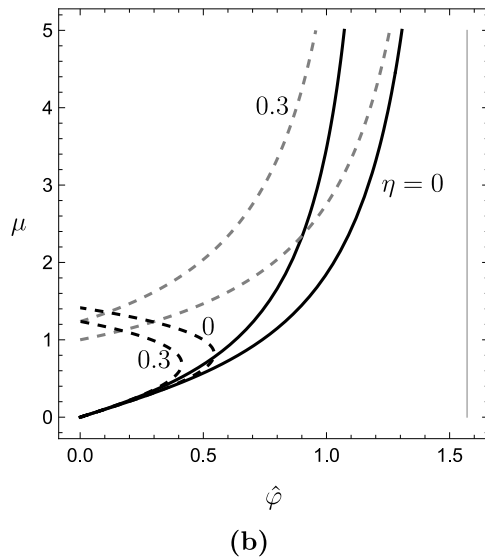
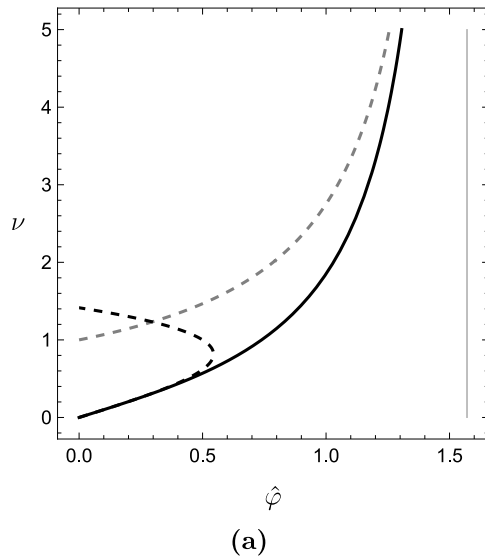


Fig. 3. Fundamental paths for: (a) $\mu = 0$ (couple acting), (b) $\nu = 0$ (force acting), for different values of $\eta = (0, 0.3)$; exact (continuous lines), asymptotic for small loads (dashed black lines), asymptotic for large loads (dashed gray lines).

4. Linear bifurcation analysis

A linear bifurcation analysis is performed. By linearized Eqs. (7)b,c around the fundamental path, one gets:

$$\begin{bmatrix} \beta + \mu \sin \hat{\varphi} & -\mu \eta \sin \hat{\varphi} + \nu \cos \hat{\varphi} \\ -\mu \eta \sin \hat{\varphi} + \nu \cos \hat{\varphi} & \alpha + \mu \eta \cos \hat{\varphi} + \nu \sin \hat{\varphi} \end{bmatrix} \begin{pmatrix} \psi \\ \theta \end{pmatrix} = \begin{pmatrix} 0 \\ 0 \end{pmatrix} \quad (15)$$

whose solutions provide the bifurcation loads and the critical modes. Two distinct analyses are carried out, in which: (i) the precritical deflection $\hat{\varphi}$ is neglected, according to the classic theory and, (ii) $\hat{\varphi} = \hat{\varphi}(\mu, \nu)$ is correctly accounted for, according to the exact theory.

4.1. Classic theory: bifurcation from the trivial path

By taking $\hat{\varphi} = 0$ in Eq. (15), these reduce to:

$$\begin{bmatrix} \beta & \nu \\ \nu & \alpha + \mu \eta \end{bmatrix} \begin{pmatrix} \psi \\ \theta \end{pmatrix} = \begin{pmatrix} 0 \\ 0 \end{pmatrix} \quad (16)$$

whose characteristic equation is:

$$\beta(\alpha + \mu \eta) - \nu^2 = 0 \quad (17)$$

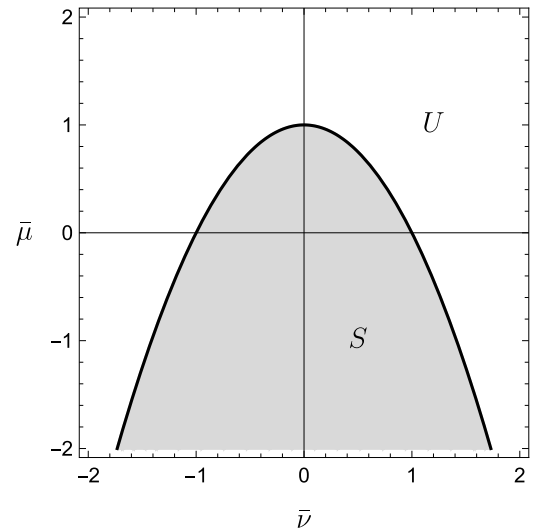


Fig. 4. Stability domain in the classic theory; S stable region, U unstable region.

When $\mu = 0, \nu \neq 0$ (i.e., the pendulum is solicited only by the couple), the previous equation supplies:

$$\nu_c = \pm \sqrt{\alpha \beta} \quad (18)$$

which is the discrete counterpart of the *Prandtl critical load* of a fixed-free elastic beam [9]. The corresponding buckling mode is of flexural-torsional type, i.e., $(\psi_c, \theta_c) = \left(1, \mp \sqrt{\frac{\beta}{\alpha}}\right)$.

When $\mu \neq 0, \nu = 0$ (i.e., the pendulum is solicited only by the force), this enters the characteristic equations only when applied eccentrically with respect the centroid B (i.e., when $\eta \neq 0$); in this case:

$$\mu_c = -\frac{\alpha}{\eta} \quad (19)$$

i.e., a bifurcation occurs only when: (i) $\eta < 0$ and P is upward, or (ii) $\eta > 0$ and P is downward. When $|\eta| \rightarrow 0$, then $|P_c| \rightarrow \infty$. The associate buckling mode is purely torsional, i.e., $(\psi_c, \theta_c) = (0, 1)$. This result differs from that relevant to the elastic beam, since, due to the rigidity of the pendulum and the arrangement of the springs, the torsional moment with respect the current axis \mathbf{a}_y is zero if $\eta = 0$, and, moreover, the bending moment with respect $\hat{\mathbf{a}}_y$ is also zero, if $\varphi = 0$ (Fig. 1b).

When $\mu \neq 0, \nu \neq 0$, i.e., force and couple act simultaneously, Eq. (17) describes the boundary of a stability domain of equation $\bar{\mu} = 1 - \bar{\nu}^2$, where $\bar{\mu} := -\frac{\eta \mu}{\alpha}, \bar{\nu} := \frac{\nu}{\sqrt{\alpha \beta}}$ (Fig. 4). It is seen that the force reduces the modulus of the Prandtl critical load when $\bar{\mu} > 0$ (i.e., when it has a destabilizing effect), or increases the critical load when $\bar{\mu} < 0$ (i.e., when it has a stabilizing effect).

4.2. Bifurcation from a nontrivial path

The Eq. (15) is considered again with no approximations. At the bifurcation, the determinant of the matrix vanishes, i.e., the following bifurcation condition holds:

$$\begin{aligned} &(\beta + \mu \sin \hat{\varphi})(\alpha + \mu \eta \cos \hat{\varphi} + \nu \sin \hat{\varphi}) \\ &- (-\mu \eta \sin \hat{\varphi} + \nu \cos \hat{\varphi})^2 = 0 \end{aligned} \quad (20)$$

to be satisfied together with Eq. (8), which describes the fundamental path. The cases of small and large in-plane rotations are discussed separately.

Small in-plane rotations. If the pendulum is out-of-plane soft, it is expected that buckling occurs at low values of the in-plane rotation (i.e., $\hat{\varphi}$ is small, but not zero). In this conditions, the results of the perturbation theory can be applied. By expanding in series the circular

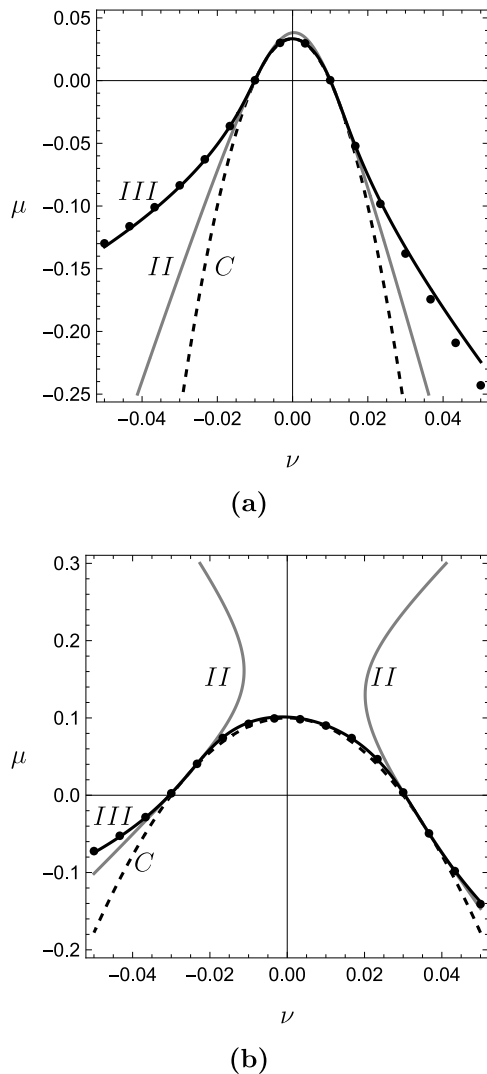


Fig. 5. Stability domain of stiff pendulums; quadratic (gray line) and cubic (black line) approximations; classic solution (dashed line); exact numerical solutions (bullets). (a) $\alpha = \beta = 0.01$, $\eta = -0.3$. (b) $\alpha = \beta = 0.03$, $\eta = -0.3$.

functions, and using for $\hat{\varphi}$ the asymptotic solution in Eq. (11), the bifurcation condition Eq. (20) reads:

$$\beta(\alpha + \eta\mu) - \nu^2 + (\mu + \nu)(\alpha\mu + \beta\nu) - \frac{1}{2}\eta\mu(\mu + \nu)[(2\alpha + \beta - 2)\mu + (3\beta - 4)\nu] = 0 \quad (21)$$

which describes a geometrical locus in the (μ, ν) plane. This is plotted in Fig. 5 for selected values of the parameters. In the same figure, exact numerical results and those of classic theory are also reported. The intersections of the locus with axes are:

$$\nu_c = \pm \sqrt{\frac{\alpha\beta}{1-\beta}} \quad (22a)$$

$$\mu_c = -\frac{\alpha}{\eta} \left(1 + \frac{\alpha^2}{2\eta^2} + \frac{\alpha^3}{\beta\eta^2} \right) + \dots \quad (22b)$$

which provide a (rough) approximation of the critical loads accounting for the precritical deflection. These, however, show that the results of the classic theory (Eqs. (18), (19)) are lower bounds for the critical loads of the nonlinear theory. Therefore, precritical deflection increase the critical load, according to the same considerations made for the fundamental path.

Large in-plane rotation: loads acting separately. When the pendulum is sufficiently out-of-plane stiff, bifurcation is expected to occur for large in-plane rotations. Since the asymptotic expression of the fundamental path is no longer valid, a numerical approach is needed. However, this is facilitated by the use of asymptotic expressions for large rotations, as commented ahead.

Bifurcation takes place when Eqs (8) and (20) are simultaneously satisfied, resulting in a system of two transcendental equations in the unknowns $\mu, \nu, \hat{\varphi}$, whose solution $\mu = \mu(\hat{\varphi})$, $\nu = \nu(\hat{\varphi})$ is a curve in the load parameter plane. To investigate the character of the response, the loads are first assumed to act separately. In this case, Eq. (8) is the implicit equation of a curve F describing the fundamental path and Eq. (20) of a curve B stating the bifurcation condition, both in the $(\hat{\varphi}, \mu)$ or $(\hat{\varphi}, \nu)$ planes. The intersections between F and B identify the critical bifurcation points $(\hat{\varphi}_c, \mu_c)$ or $(\hat{\varphi}_c, \nu_c)$. By varying the parameters α, β (and, moreover, η , but only in the case of force), the curve B changes, while the curve F remains unaltered, since the fundamental path does not depend on the out-of-plane stiffnesses α, β . Since the interest is focused on load parameters spanning the range from zero to infinity (to detect possible divergence), it is convenient to plot the curves as a function of μ^{-1} and ν^{-1} , in order to map infinity to zero.

In the case of the couple, the bifurcation points are solution to:

$$F : f(\hat{\varphi}, \lambda) := \lambda - \frac{\cos \hat{\varphi}}{\hat{\varphi}} = 0 \quad (23a)$$

$$B : g(\hat{\varphi}, \lambda; \alpha, \beta) := \lambda^2 \alpha \beta + \lambda \beta \sin \hat{\varphi} - \cos^2 \hat{\varphi} = 0 \quad (23b)$$

where $\lambda := \nu^{-1}$, and in the case of the force, to:

$$F : f(\hat{\varphi}, \lambda) := \lambda - \frac{\cos \hat{\varphi} - \eta \sin \hat{\varphi}}{\hat{\varphi}} = 0 \quad (24a)$$

$$B : g(\hat{\varphi}, \lambda; \alpha, \beta) := \lambda^2 \alpha \beta + \lambda \alpha \sin \hat{\varphi} + \lambda \beta \eta \cos \hat{\varphi} + \eta \sin \hat{\varphi} \cos \hat{\varphi} - \eta^2 \sin^2 \hat{\varphi} = 0 \quad (24b)$$

where $\lambda := \mu^{-1}$. It appears that $(\lambda, \hat{\varphi}) = (0, \frac{\pi}{2})$ or $(\lambda, \hat{\varphi}) = (0, \frac{\pi}{2} - \arctan(\eta))$ are solutions to the previous equations, respectively (denoted ahead as the point O of the plane), denoting an infinitely large critical load, whose physical meaning has already been commented. It is useful, for the discussion of the results, to expand F, B around O , thus obtaining:

$$F : \lambda = -\frac{2}{\pi} \epsilon + \frac{4}{\pi^2} \epsilon^2 + \dots \quad (25a)$$

$$B : \lambda = \frac{1}{\beta} \epsilon^2 + \frac{\beta - 6\alpha}{6\beta^2} \epsilon^4 + \dots \quad (25b)$$

and:

$$F : \lambda = -\frac{2\sqrt{1+\eta^2}}{\pi - 2 \arctan(\eta)} \epsilon + \frac{4\sqrt{1+\eta^2}}{(\pi - 2 \arctan(\eta))^2} \epsilon^2 + \dots \quad (26a)$$

$$B : \lambda = \frac{\eta\sqrt{1+\eta^2}}{\alpha + \beta\eta^2} \epsilon + \frac{\beta^2\eta^4(1+\eta^2)^{3/2}}{(\alpha + \beta\eta^2)^3} \epsilon^2 + \dots \quad (26b)$$

where only the branch $\lambda > 0$ of B has been considered, and $\epsilon := \hat{\varphi} - \frac{\pi}{2}$ or $\epsilon := \hat{\varphi} - \frac{\pi}{2} + \arctan(\eta)$ introduced.

In the case of the couple, the plots in Figs. 6a,b are obtained, in each of which a value of β is fixed, and several values of α are considered. According to Eq. (25), B has horizontal tangent and upward concavity at O , while F has negative slope; therefore, when α is not too large, B crosses F at two distinct points (in addition to O), so that two bifurcation points exists. When, however, for a fixed β , α exceeds a threshold value, the fourth-order terms in Eq. (25)b become significant, entailing a change of curvature causing the two curves to no longer intersect each other, so that no bifurcation points exist. The threshold value of α corresponds to the coalescence of the two crossing points, i.e., to the occurrence of a *merging*, as discussed in the

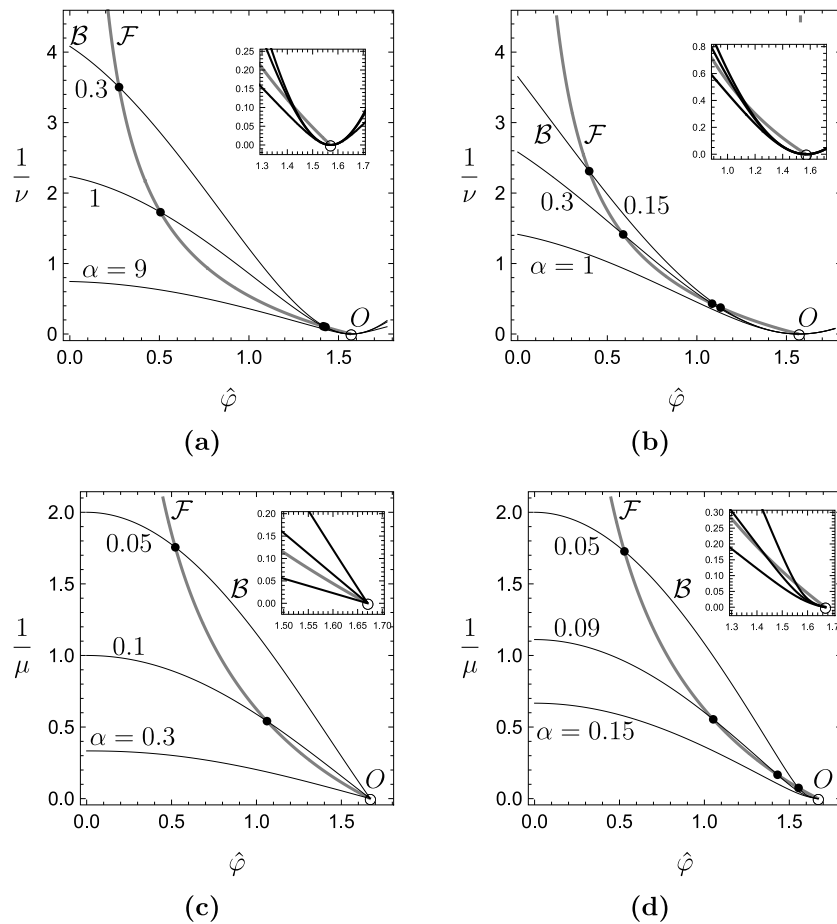


Fig. 6. Representation of the fundamental path \mathcal{F} (gray line) and bifurcation locus \mathcal{B} (black line) in the $(\hat{\varphi}, \nu^{-1})$ or $(\hat{\varphi}, \mu^{-1})$ planes. Pendulum loaded by the couple ν : (a) $\beta = 0.2$ and $\alpha = 0.3, 1, 9$; (b) $\beta = 0.5$ and $\alpha = 0.15, 0.3, 1$. Pendulum loaded by the force μ , when $\eta = -0.1$: (c) $\beta = 1$ and $\alpha = 0.05, 0.1, 0.3$; (d) $\beta = 50$ and $\alpha = 0.05, 0.09, 0.15$.

Introduction. The larger β , the flatter \mathcal{B} at O and the smaller α at which bifurcation disappears. It is concluded that, if the pendulum is loaded by the couple only, two bifurcation points or no bifurcation points exist. The bifurcation load is *finite* for soft pendulums and does not exist for stiffer pendulums. From a mechanical point of view, merging is the result of a *nonlinear interaction* between two singular points (*i.e.*, two branch points). When the pendulum is made out-of-plane stiff, the first (smaller) critical load increases, but the second (larger) critical load decreases. The first circumstance is obvious, the second is less obvious, and can only be explained mathematically. The presence of the higher critical load *prevents* the lower from tending to infinity, so that the coalescence destroys the bifurcation.

The case of the force acting alone is now analyzed. For a selected $\eta = -0.1$, the plots in Figs. 6c,d are obtained, in each of which β is fixed and several values of α are considered. Fig. 6c refers to a value of β that is not very large. It appears that, with $\eta < 0$, the slopes of \mathcal{F} and \mathcal{B} are both negative, but the (modulus) of the slope of \mathcal{B} is either larger or smaller than that of \mathcal{F} , depending on whether α is larger or smaller than a threshold value at which the two slopes are identical. When the slope of \mathcal{B} is larger in modulus, there exists a unique bifurcation point, whose associated critical load increases and continuously approaches infinity as α increases. When a threshold value of α is overcome, at which the slope of \mathcal{B} is smaller in modulus than that of \mathcal{F} , the bifurcation disappears. This is the phenomenon called *divergence*. However, when β is large (Fig. 6d), a positive contribution adds to the negative slope at O , reducing its modulus; moreover, the concavity is upward near O , then turning downward far from O , which entails the existence of two bifurcation points. Therefore, a merging may occur also for the force, when $\beta \gg \alpha$.

The previous results concerning divergence are easily explained on a mechanical ground and similarly to the merging case, the critical load increases with the out-of-plane stiffness. However, since the pendulum experiences large in-plane rotation, the O point is approached and, in the limit process, reached at a certain value of the stiffness. Further increments of stiffness have no practical effect on bifurcation, as the O point is reached. The same phenomenon can be commented on in an alternative way, by saying that, once the out-of-plane stiffnesses have been fixed, the softer the in-plane stiffness, the larger the critical load. This latter is the common point of view in the literature concerning divergence. However, it is important to say that the two phenomena, divergence and merging, can be viewed from a different perspective, as the same phenomenon, as discussed in what follows.

Some diagrams collecting the results so far discussed are shown in Fig. 7. They show the critical loads μ_c, ν_c vs the stiffness α , for fixed β (and possibly η); moreover, labeled dots indicate the rotation $\hat{\varphi}_c$ at bifurcation. Figs. 7a,b refer to the couple, Figs. 7c,d to the force; the parameters β and η are the same chosen in Fig. 6, respectively. The results of the classic theory are also reported for comparison, which are valid only for very small α , for which bifurcation manifests with small precritical nonlinearities. When the pendulum is loaded by the couple (Figs. 7a,b) the merging phenomenon appears for any β at large $\hat{\varphi}_c$. When the pendulum is loaded by the force, it needs to distinguish: for the smaller β a divergence occurs (at which $\hat{\varphi}_c$ tends to $\frac{\pi}{2} - \arctan(\eta)$); for the larger β a merging manifests itself (again at large $\hat{\varphi}_c$).

The previous discussion suggests the opportunity to find the locus $h(\alpha, \beta) = 0$ which separates, in the plane of parameters, the regions in which Eqs. (23), (24) admit two, one or zero *finite* solutions, denoting the existence of a merging, divergence or stable systems, respectively.

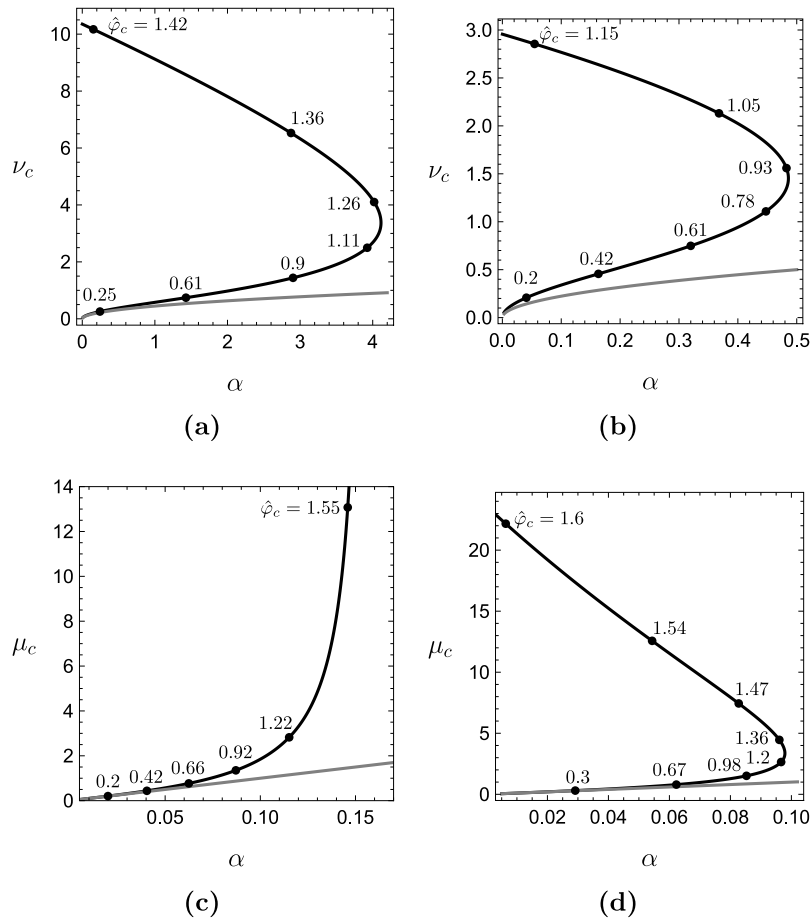


Fig. 7. Critical loads μ_c, ν_c vs the torsional stiffness α . Pendulums loaded by a couple: (a) $\beta = 0.2$, (b) $\beta = 0.5$; pendulums loaded by a force when $\eta = -0.1$: (c) $\beta = 1$, (d) $\beta = 50$. Exact results (black line), classic theory (gray line). Labeled dots indicate the in-plane rotation at bifurcation.

- The curve which bounds the region in which the equations admit two roots (existing both in the case of the couple and in that of the force), is determined by the condition that the loci \mathcal{F}, \mathcal{B} are tangent at their intersection point. The condition of tangency is expressed by the zeroing of the determinant of the Jacobian matrix, i.e.:

$$\begin{vmatrix} \frac{\partial f}{\partial \hat{\varphi}} & \frac{\partial f}{\partial \lambda} \\ \frac{\partial g}{\partial \hat{\varphi}} & \frac{\partial g}{\partial \lambda} \end{vmatrix} = 0 \quad (27)$$

with f, g defined in Eqs. (23) or (24). By appending Eq. (27) to Eqs. (23) or (24), and assuming α, β as free parameters (with η fixed), a system of three transcendental equations in the four unknowns $\hat{\varphi}, \lambda, \alpha, \beta$ is obtained. A path-following numerical algorithm is used to find the solution $\hat{\varphi}(s), \lambda(s), \alpha(s), \beta(s)$, with s a parameter, which, in particular, describes the curve $\alpha = \alpha(s), \beta = \beta(s)$ sought for. The curve separates the plane in two regions: in that containing the origin there are two roots, in the other region zero roots.

- The curve which bounds the region of existence of just one root (case occurring only in the case of the force), it is determined by the condition of tangency of the loci \mathcal{F}, \mathcal{B} at the point O . By using the expressions of the derivatives of \mathcal{F} and \mathcal{B} with respect to $\hat{\varphi}$ at O (i.e., Eq. (26)), a closed-form expression is found, i.e.:

$$\alpha + \beta \eta^2 + \left(\frac{\pi}{2} - \arctan(\eta) \right) \eta = 0 \quad (28)$$

The curve separates the plane in two regions: in that containing the origin there exist just one roots, in the other region zero or two roots. Indeed, when \mathcal{B} has at O a slope in modulus smaller

than \mathcal{F} , then \mathcal{B} can either cross \mathcal{F} two times (for smaller α) or zero times (for larger α), as Fig. 6d shows.

The curves thus obtained are plotted in the bifurcation charts in Fig. 8. Fig. 8a refers to the couple, Fig. 8b to the force. A sketch of the curves \mathcal{F} and \mathcal{B} , holding in each of the regions in which the plane is separated, is also shown. The unique curve in Fig. 8a is the locus of systems for which two critical load $\nu_{c1} = \nu_{c2}$ coalesce, i.e., a merging locus; the lower region represents systems for which two, but distinct, critical loads exist, $\nu_{c1} < \nu_{c2}$; the upper region represents *unconditionally stable* systems, for which bifurcation does not manifest at all (i.e., it disappears). In Fig. 8b a new curve adds itself to the merging loci, at which *one of the roots goes to infinity*. Thus three regions are identified. System falling in the lowest one (one root) possess a unique critical load μ_{c1} ; systems in the highest region (zero roots) are unconditionally stable. System in the intermediate region (two roots) possess two critical loads, $\mu_{c1} < \mu_{c2}$, which coalesce at the upper boundary, and one of which, μ_{c2} , tends to infinity at the lowest boundary.

To better explain the phenomenon, three families of systems, labeled I, II, III in Fig. 9a, loaded by the force are considered, in which β is fixed and α is progressively increased. The significant values $\alpha_0, \alpha_1, \alpha_2, \alpha_3$ are indicated, at which the horizontal paths cross the boundaries of the bifurcation. The relevant curves displaying the critical load μ_c vs α are plotted in Fig. 9b. Along path I (corresponding to a value of β sufficiently large), two critical loads exist, coalescing at α_0 , and then disappear; merging is thus explained. Along path II (corresponding to an average value of β), when $\alpha < \alpha_1$, a low critical load μ_{c1} exists; however, when α_1 is just exceeded, a second higher critical load μ_{c2} (stemming from infinity) appears; when α is further increased, the two critical loads approach each other, coalesce at α_2 and then disappear.

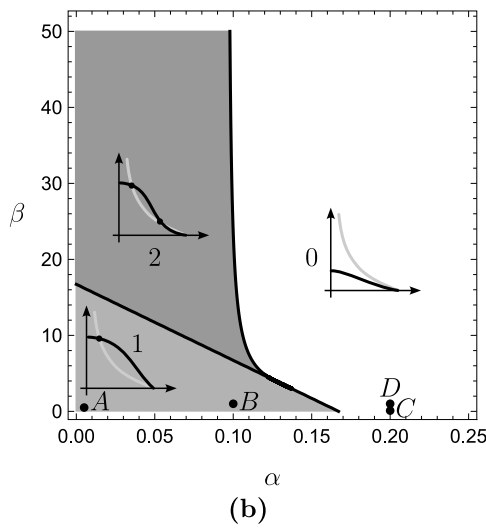
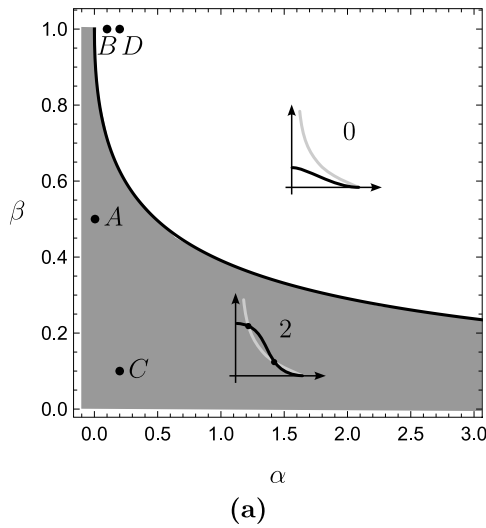


Fig. 8. Bifurcation charts in the stiffness parameter plane: (a) pendulum loaded by a couple, (b) pendulum loaded by a force ($\eta = -0.1$). Number of bifurcation points (0,1,2) in each region and relevant curves \mathcal{F} (gray) and \mathcal{B} (black).

Thus, again, the mechanism of merging is detected, although different from the “classical” one relevant to path I, since the higher bifurcation load only appears when the stiffness is sufficiently large. This kind of merging could be classified as an “interaction among a finite and an infinitely large critical loads”, which merge at a finite merging load. Finally, path III (which corresponds to a low value of β), a mechanism similar to that on path II occurs, but where the smaller critical load now approaching the larger critical load, so that divergence takes place. The mechanism clarifies that *divergence should be meant as a merging at infinity*. According to this reading, merging is always the basic mechanism leading to buckling disappearance. It, however, can manifest at a finite value of load (the properly said merging), or at an infinitely large value (the usually called divergence), which involve coalescence between two large critical loads. This aspect is believed to be the most important result of this study.

Large in-plane rotation: loads acting simultaneously. When the two loads act simultaneously, Eqs. (8) and (20) must be solved for the two unknown bifurcation parameters (μ_c, ν_c) and the critical rotation $\hat{\varphi}_c$. Therefore, for any fixed mechanical and geometric characteristics, there exist ∞^1 critical states. By parameterizing them by ν (or by μ), the parameter μ (or ν) is eliminated between the two equations. By

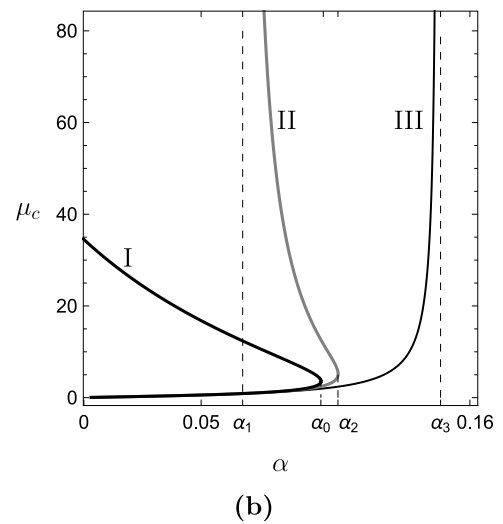
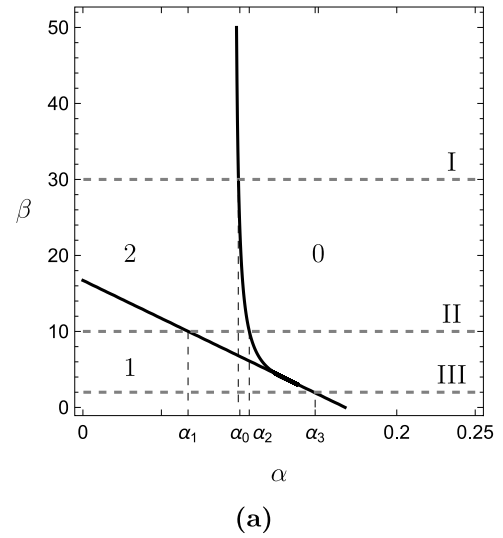


Fig. 9. Critical loads μ_c vs the torsional stiffness α for three fixed values of the out-of-plane flexural stiffness β , as denoted in sub (a): (a) families of systems; (b) relevant critical loads denoting: (I) merging between two finite critical loads, (II) merging at a finite value of a large and a small critical load, (III) divergence, i.e., merging at infinite between two large critical loads.

assigning to $\nu = \nu_c$ (or $\mu = \mu_c$) a set of values, the corresponding $\hat{\varphi} = \hat{\varphi}_c$ is determined by numerically solving the resulting equation. With the pairs $(\nu_c, \hat{\varphi}_c)$ (or $(\mu_c, \hat{\varphi}_c)$) known, the eliminated parameter is evaluated from Eq. (8).

To investigate the combined effect of the two loads, four systems, labeled as A, B, C, D are considered, whose stiffnesses α, β are the coordinates of the homonym points marked in the bifurcation chart of Fig. 8, namely: system A instabilizes both for the force $\mu > 0$ and the couple $\pm \nu$ acting separately; system B instabilizes for the sole force, but is unconditionally stable when loaded by the sole couple; system C behaves in the opposite way, i.e., instabilizes for the sole couple, but is unconditionally stable when loaded by the sole force; finally, system D is unconditionally stable both for the force and the couple acting separately. The relevant stability domains are plotted in Fig. 5.

System A (Fig. 10a) behaves as already illustrated in Fig. 5; it appears that a negative force has a stabilizing effect, since increases the critical value of the couple, while a positive force has a destabilizing effect. However, a small positive couple has a beneficial effect on the

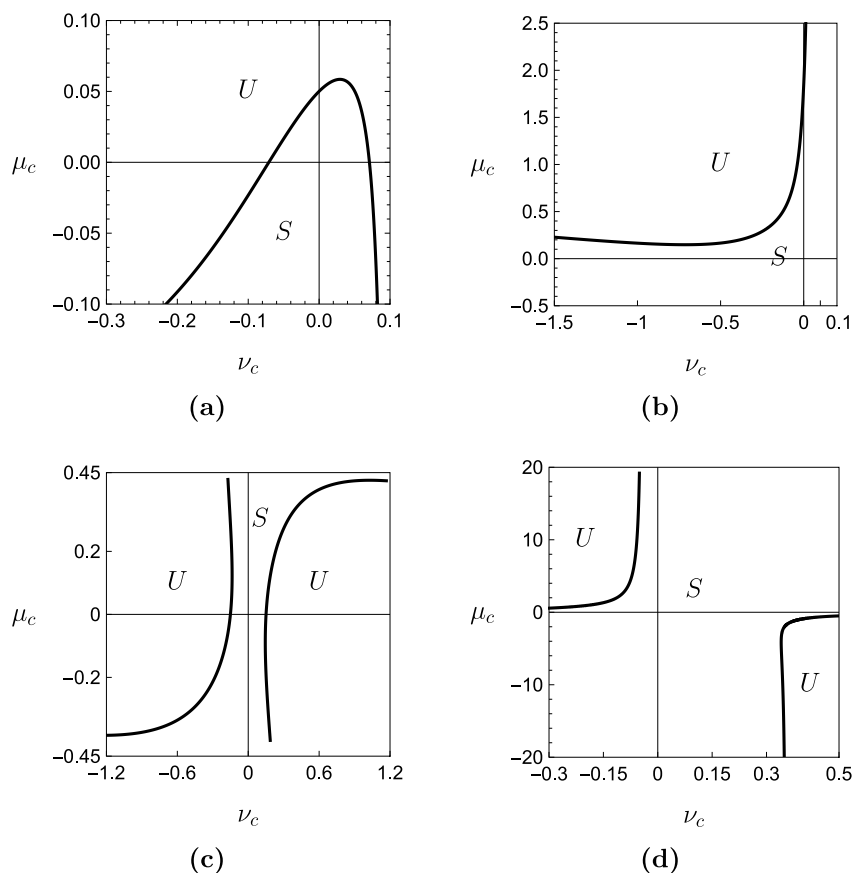


Fig. 10. Exact stability domains for $\eta = -0.1$ and: (a) system A, $\alpha = 0.005$, $\beta = 0.5$, (b) system B, $\alpha = 0.1$, $\beta = 1$, (c) system C, $\alpha = 0.2$, $\beta = 0.1$, (d) system D, $\alpha = 0.2$, $\beta = 1$; points A, B, C, D marked in Fig. 8.

force, since the maximum μ_c is larger of the value corresponding to $\nu = 0$. System B has a completely different shape, since the domain modifies the convexity and its boundary no longer crosses the ν_c axis. Positive couples have a beneficial effect on buckling triggered by the sole force; negative couples have a destabilizing effect. System C is the counterpart of system B, since the domain boundaries do not cross the μ_c axis. Such boundaries are defined by two curves which cross the ν_c axis at equal and opposite values. Positive (negative) forces have a beneficial effect on the positive (negative) critical couple, while leaving almost unaltered the negative (positive) critical couples. System D is stable for forces and couples falling in the first and third quadrants. It becomes unstable at curves lying in the second and fourth quadrants, which tend asymptotically to the coordinate axes.

5. Conclusions and perspectives

The phenomenon of the buckling disappearance in nonlinear systems affected by precritical nonlinearities has been investigated, referring to a three degree-of-freedom spherical pendulum, constrained by linear elastic springs. Such a system, loaded by a transverse force and/or a conservative couple, undergoes an in-plane deflection, followed by a lateral buckling of flexural-torsional type. It has been shown that, by suitably varying the torsional and out-of-plane stiffness, the system exhibits either *merging* or *divergence*, i.e: (i) it buckles, at a finite value of the load, when the out-of-plane stiffness is sufficiently small, or (ii) it buckles at an infinitely large (in modulus) loads at a threshold value of the stiffness, respectively. In both cases, the system is unconditionally stable when stiffness is high. Indeed, if the pendulum is out-of-plane stiff, large in-plane deflections precede buckling, by reducing the arm of the transverse force and/or the arm of the conservative couple, so that buckling cannot take place. The following conclusions can be drawn.

1. Divergence and merging can coexist in the same mechanical system; the occurrence of one of the two forms depend on how the geometrical and physical parameters are varied, as well as on the type of load. However, since the behavior is governed by nonlinear transcendental equations, the results cannot be predicted by a qualitative analysis.
2. Merging occurs when two finite critical load coalesce; divergence occurs when a finite critical load approaches an infinitely large critical load. In this respect, the two phenomenon are the results of the same mechanism. A smooth transformation from one to the other mechanism has been shown to exist.
3. Divergence does exist in system with linear constitutive law. Results of literature, showing that merging can be changed into divergence by passing from linear to nonlinear elasticity, confirm the results stated in the previous items.
4. Precritical nonlinearities, in case of linear elasticity, usually have a beneficial effect on buckling, since they reduce the destabilizing effect of loads, via the change of geometry, possibly leading to the disappearance of buckling.
5. The combined effect of two forces can be further beneficial, leading to stability domains, in the plane of the load multipliers, which do not intersect one or both the two axes.

The previous results are believed to be useful to more extensive investigations relevant to continuous, rather than discrete, systems. Moreover, the influence of different types of elastic laws deserves attention. Finally, the whole analysis should be pushed forward to analyze the postbuckling behavior, either by determining the bifurcated branches, when existing, or possible external (to the fundamental path) branches, but close to it.

CRediT authorship contribution statement

Angelo Luongo: Writing – review & editing, Methodology, Investigation, Conceptualization, Supervision. **Manuel Ferretti:** Writing – review & editing, Methodology, Investigation, Conceptualization, Software.

Declaration of competing interest

The authors declare that they have no known competing financial interests or personal relationships that could have appeared to influence the work reported in this paper.

Data availability

Data will be made available on request.

References

- [1] S. Yiatros, M.A. Wadee, Interactive buckling in sandwich beam-columns, *IMA J. Appl. Math.* 76 (1) (2011) 146–168.
- [2] G. Piana, E. Lofrano, A. Manuella, G. Ruta, A. Carpinteri, Compressive buckling for symmetric TWB with non-zero warping stiffness, *Eng. Struct.* 135 (2017) 246–258.
- [3] Y. Su, H. Zhao, S. Liu, R. Li, Y. Wang, Y. Wang, J. Bian, Y. Huang, Buckling of beams with finite prebuckling deformation, *Int. J. Solids Struct.* 165 (2019) 148–159.
- [4] H. Zhao, Y. Su, Buckling of bulk structures with finite prebuckling deformation, *J. Appl. Mech.* 89 (5) (2022) 051006.
- [5] S. Palumbo, L. Deseri, D.R. Owen, M. Fraldi, Disarrangements and instabilities in augmented one-dimensional hyperelasticity, *Proc. R. Soc. A: Math. Phys. Eng. Sci.* 474 (2218) (2018) 20180312.
- [6] M. Fraldi, S. Palumbo, A. Cutolo, A.R. Carotenuto, F. Guarracino, On the equilibrium bifurcation of axially deformable holonomic systems: solution of a long-standing enigma, *Proc. R. Soc. A* 477 (2253) (2021) 20210327.
- [7] V.I. Feodosiev, *Advanced Stress and Stability Analysis: worked Examples*, Springer Science & Business Media, 2005.
- [8] M. Ferretti, S. Di Nino, A. Luongo, A paradigmatic system for non-classic interactive buckling, *Int. J. Non-Linear Mech.* 134 (2021) 103735.
- [9] A. Luongo, M. Ferretti, S. Di Nino, *Stability and Bifurcation of Structures: Statical and Dynamical Systems*, Springer Nature, 2023.
- [10] D. Bigoni, F. Bosi, F. Dal Corso, D. Misseroni, Instability of a penetrating blade, *J. Mech. Phys. Solids* 64 (2014) 411–425.
- [11] F. Bosi, D. Misseroni, F. Dal Corso, S. Neukirch, D. Bigoni, Asymptotic self-restabilization of a continuous elastic structure, *Phys. Rev. E* 94 (6) (2016) 063005.
- [12] Q. Li, T.J. Healey, Stability boundaries for wrinkling in highly stretched elastic sheets, *J. Mech. Phys. Solids* 97 (2016) 260–274.
- [13] A.A. Sipoș, E. Fehér, Disappearance of stretch-induced wrinkles of thin sheets: a study of orthotropic films, *Int. J. Solids Struct.* 97 (2016) 275–283.
- [14] T. Wang, C. Fu, F. Xu, Y. Huo, M. Potier-Ferry, On the wrinkling and restabilization of highly stretched sheets, *Internat. J. Engrg. Sci.* 136 (2019) 1–16.
- [15] A. Luongo, M. Ferretti, Beneficial effects of the precritical nonlinearities on the lateral buckling of extremely flexible beams, *Int. J. Non-Linear Mech.* 159 (2024) 104593.
- [16] M. Epstein, *A buckling question*, 2022, arXiv preprint arXiv:2211.14689.
- [17] D. Zaccaria, D. Bigoni, G. Noselli, D. Misseroni, Structures buckling under tensile dead load, *Proc. R. Soc. A: Math. Phys. Eng. Sci.* 467 (2130) (2011) 1686–1700.
- [18] A.V. Perelmuter, V. Slivker, *Handbook of Mechanical Stability in Engineering: General Theorems and Individual Members of Mechanical Systems*, World Scientific, 2013.
- [19] A. Luongo, D. Zulli, *Mathematical Models of Beams and Cables*, John Wiley & Sons, 2013.